Modelling and Analysis of an Offshore Oscillating Water Column Wave Energy Converter

David P. Cashman[1], Dara L. O' Sullivan[2], Michael G. Egan[1] and John G. Hayes[1]

[1]Department of Electrical and Electronic Engineering,
University College Cork,
Ireland.
E-mail: davidpc@rennes.ucc.ie,m.egan@ucc.ie,john.hayes@ucc.ie
[2]Hydraulics and Maritime Research Centre,
University College Cork,
Ireland.
E-mail: dara.osullivan@ucc.ie

Abstract

This paper investigates the modelling of a quarter scale offshore oscillating water column (OWC) wave energy converter (WEC) with results from a prototype device used to validate the model. The OWC WEC utilises a specialised bi-directional air turbine known as the Wells turbine. The paper investigates the modelling of this turbine and studies the electrical output from a generator to be coupled to the turbine. Simulations of the proposed system are carried out under multiple sea state conditions and are compared to results from the prototype device located at an experimental test site in Ireland.

Keywords: Electical Machines, Device Control, Wells Turbine Modelling

Nomenclature

Ψ	=	Non-dimensional pressure coefficient
p	=	Pressure head in the buoy chamber
ρ_a	=	Air density
N	=	rotational speed in rads/s
D	=	Diameter of Wells turbine
Φ	=	Non-dimensional flow coefficient
Q	=	Axial flowrate
A_A	=	Annular Area
A_C	=	Chamber Area
U_t	=	Tip velocity
Π	=	Non-dimensional power coefficient
T_{ND}	=	Non-dimensional torque
η	=	Efficiency
B_t	=	Damping coefficient
B_r	=	Damping ratio
I_a	=	Armature Current
V_a	=	Armature Voltage
B_m	=	DC machine friction factor
V_c	=	Capacitor Voltage
T_{mech}	=	Mechanical Torque
T_{em}	=	Electromagnetic Torque
T_f	=	Frictional Torque
T_j	=	Inertial Torque
P_{elec}	=	Electrical Power
P_{eloss}	=	Electrical Power Losses
P_{mloss}	=	Mechanical Power Losses
P_{pneu}	=	Pneumatic Power

1 Introduction

The increased use of renewable energy technologies in electrical generation systems worldwide is well documented. Wind power generation is the most mature technology and is therefore the most widely used. In recent times wave energy has acquired a large interest. The potential for power extraction is very significant. In Western Europe the power density of the resource in the seas are estimated to be 33 kW/m in Southern regions such as Portugal ranging up to 75 kW/m off Scotland [1]. A recent study estimated that the annual potential power off the coast of Ireland is in the region of 59 TWh [2].

This potential has led to various technologies being proposed for wave energy converters (WEC). These technologies include heaving body converters, over topping devices, floating hinged devices and oscillating water column devices. A summary of the device types is discussed in [3]. Many of these devices have been developed to pre-commercial prototypes and the progress a number of them are variously discussed in [4]-[6].

Of all the proposed technologies the oscillating water column (OWC) is the most advanced [7]. Working shore based protoypes have been developed in Scotland [8] and Portugal [9], [10] however there is a current emphasis on developing offshore devices as the potential for power extraction is much greater.

Considerable challenges exist for the electrial conversion system in an offshore OWC WEC. Some of the key problems faced are the oscillatory nature of the power profile of the sea and also the harsh conditions that exist in this environment. In [11]-[14] the reduction of large power fluctuations feeding to the grid is explored in different methods.

The selection of the electrical generator is crucial for any successful WEC to be developed. The advantages and disadvantages of each of the main generator types are investigated in [15].

The OWC WEC utilises a relatively high speed bi-directional air turbine known as the Wells turbine and this type of setup has been modelled previously in [16]. This paper presents the turbine and seeks to develop a model for the turbine. Actual experimental data obtained from a quarter scale prototype device is used to develop the characteristic non-dimensional torque curve for the device. Simulations of the device coupled to an electrical generation system are carried out with the results compared to the actual prototype data for validation purposes.

The OWC WEC is introduced in Section 2. Section 3 discusses the mathematical model used for the Wells turbine. Section 4 outlines the experimental test system. Section 5 outlines the development of the simulation model for the device. The simulated results obtained using the electrical system are compared to the experimental results in Section 6.

2 OWC wave energy converters

The OWC WEC utilises a three step conversion process where energy in the sea is converted to aerodynamic energy that is transformed to mechanical energy via an air turbine which is in turn converted to electrical power via a rotary electrical generator. The Wells turbine is a bi-directional air turbine and is thus far the most popular choice for operation in an OWC application. The operation of this turbine is discussed in more detail in Section 3.

The OWC WEC operates on the principle of water in the column rising and falling as the waves in the sea excite motion in the buoy type structure. In Fig. 1 it can be seen that in the case where the water level in the column rises, relative to the buoy, the air in the buoy chamber is pushed out to the atmosphere. This outflow of air is used to rotate the turbine to convert the pneumatic power to mechanical power. The aerodynamic and thermodynamic principles involved in this process are beyond the scope of this paper but can be found in [17].

The alternative motion is when the water inside the column falls causing air from the atmosphere to be pulled into the resulting vacuum in the buoy chamber. This airflow can again be converted to mechanical form via a turbine. The inflow and outflow motion of the air occurs once per sea wave cycle and it is for this reason that the Wells turbine is well suited to the OWC application. The symmetrical nature of the Wells Turbine is an important attribute to convert the power from the reciprocating airflow.

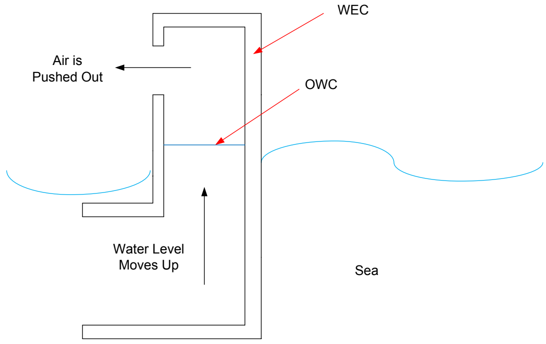

Figure 1: OWC operation

3 Wells turbine modelling

As has been mentioned previously the Wells turbine is well suited to OWC applications due to its bi-directional characteristic. The turbine itself has no moving parts as its blades are generally fixed making it attractive from a maintenance point of view. Pitching blade Wells turbines are available to increase efficiency but are not widely used due to the maintenance costs associated with them.

The Wells turbine is generally represented in non-dimensional form as this is a more convenient manner of characterising its aerodynamic properties. The following expressions from [10] and [8] denote the non-dimensional (ND) quantities:

$$\Psi = \frac{p}{\rho_a N^2 D^2} \tag{1}$$

$$\Phi = \frac{Q}{A_a U_t} \tag{2}$$

$$\Pi = \frac{P_t}{\rho_a N^3 D^5} \tag{3}$$

It has been shown in [10] that Ψ has a linear relationship with Φ for a fixed turbine speed N. The slope of this line is known as the applied damping and this is denoted B_A. If an electrical analogy is used B_A could be considered the resistance, Ψ would be applied voltage and Φ would be current.

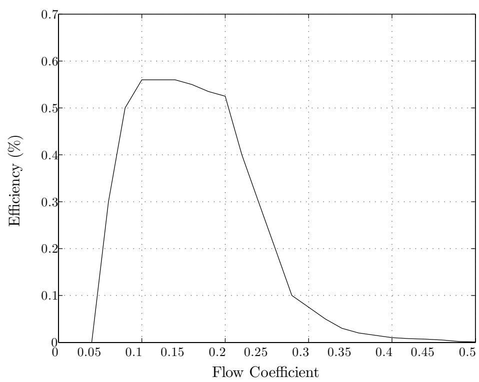

Figure 2: Wells Turbine Efficiency Characteristic

In [8] an efficiency characteristic of the Wells turbine as a function of ND flow Φ is given. This characteristic is plotted in Fig. 2. It can be seen from the plot that a peak efficiency of 56% is achieved at a flow coefficient of approximately 0.15. This point corresponds to when the WEC operates with an optimal flow regime. As the flow rate increases aerodynamic stall occurs in the turbine and its efficiency rolls off significantly. Finally at lower flow rates the efficiency initially drops off slowly before a significant drop off occurs at very low flow coefficient. It can be seen from Fig. 2 that zero efficiency does not correspond to zero flow.

At flow coefficient rates close to zero the efficiency of the turbine is negative due to frictional and stiction losses. This highlights the characteristic that the Wells Turbine is non-self starting. The turbine must therefore be spun by an external torque source up to a threshold speed before it can begin converting pneumatic power to mechanical power.

Taking the efficiency characteristic shown in Fig. 2 it is possible to develop a non-dimensional torque characteristic for the Wells turbine. This characteristic fully predicts the turbine's performance from low flow rates to stall. The ND Torque equation can be derived using (3):

$$T_{ND} = \frac{T}{\rho_a N^2 D^5} \tag{4}$$

The development of the non-dimensional torque characteristic is discussed in a later section.

4 Experimental Test System Description

The development of the turbine model was based on experimental data obtained from a quarter scale offshore OWC WEC located at the Irish test site. The system consists of a Wells turbine coupled to a dc electrical generator. The electrical generator is driven by a dc-dc converter that is controlled to maintain the speed of the system at a specified value. The controller gains are set to allow the speed to vary +/- 20% about the setpoint value. Finally a load resistance is connected to the system to dissipate the electrical power generated from the system. A block diagram of the system is shown in Fig. 3.

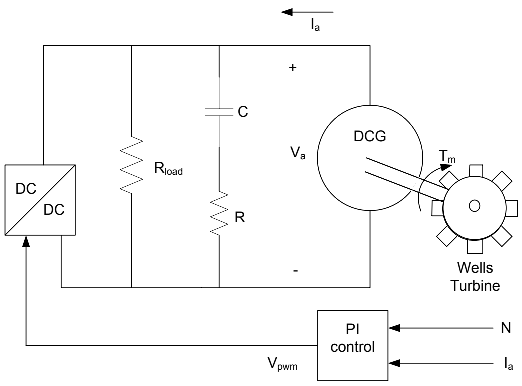

Figure 3: Electrical Generation System

4.1 Measurement of Electrical and Mechanical Parameters

The electrical system used was tested on-site and the key parameters of the dc generator were established. These parameters included total machine and turbine inertia, J, machine friction factor, B_m, machine constant, k_t and machine armature resistance R_a.

The electrical system sampled machine voltage, V_a, current, I_a and rotational speed, N, at a a sampling time of 0.2 s. By using these measured electrical parameters at each time interval it was possible to estimate the mechanical shaft torque delivered to the system from the Wells turbine. The mechanical torque is given by the following equation:

$$T_{mech}(t) = T_{em}(t) + T_f(t) + T_j(t) \tag{5}$$

where T_{em}, T_f and T_j are the generated electromagnetic, frictional and inertial torques respectively. These torques can be obtained at each time sample using the following equations:

$$T_{em}(t) = \frac{P_{elec}(t) + P_{eloss}(t)}{N(t)} \tag{6}$$

$$T_f(t) = B_m N(t) \tag{7}$$

$$T_j(t) = J\frac{dN(t)}{dt} \tag{8}$$

where P_{elec} is the generated electrical power and P_{eloss} is the machine electrical losses. P_{elec} is determined by the product of armature voltage and current and P_{eloss} is the power loss in the armature resistance of the machine.

The non-dimensional torque can then be obtained by using (4).

4.2 Measurement of Pnuematic Parameters

In a similar method to that which has been discussed for the torque, by using the measured pressure within the OWC chamber and turbine damping ratio it is possible to derive the non-dimensional flow. The pressure within the chamber was measured using a calibrated +/- 200 mbar vented guage pressure sensor and was again sampled at a rate of 0.2 s. The flow inside the chamber was derived using turbine damping from the following equation:

$$Q(t) = \frac{p(t)}{B_t(t)} \tag{9}$$

where the applied damping B_t is given by the following expression:

$$B_t(t) = \frac{2\rho_a D N(t) B_r}{A_A} \tag{10}$$

in which B_r is the damping ratio of the turbine and is defined as:

$$B_r = \frac{\Psi}{\Phi} \tag{11}$$

The damping ratio was calculated from complex fluid dynamic analysis based on turbine design specifications.

5 Development of ND torque profile

As has been discussed previously the Wells turbine can be modelled using an efficiency curve that denotes the regions of operation for the turbine. This can be further developed to give a non-dimensional torque profile that predicts the mechanical torque output from the turbine based on the flow conditions it experiences.

With the instantaneous non-dimensional flow and torque of the system defined from the method described in the previous section it was then possible to develop the non-dimensional characterisic curve. The equations for non-dimensional quantities assume that the speed of the system was constant and therefore the data was sorted into a series of speed bins of 20 RPM intervals.

A family of scatter diagrams for non-dimensional torque versus non-dimensional flow for the various speed profiles were then developed.

The non-dimensional torque data was then divided into groups in intervals of 0.02 in flow coefficient. The mean of the non-dimensional torque in each group was taken allowing for characteristic curves of non-dimensional torque versus flow coefficient for the Wells turbine to be produced. A sample of the results are shown in Fig. 4 where the speed range is 1770-1890 RPM.

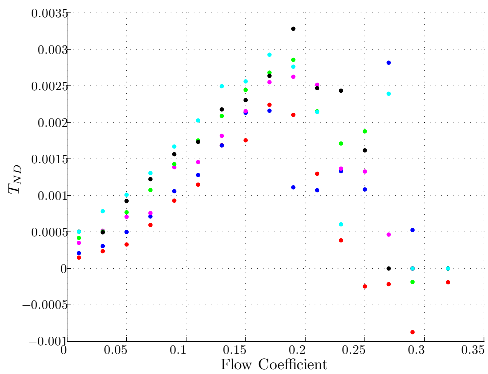

Figure 4: Scatter Plot of ND Torque vs Flow coefficient

Some variation in the curves was still found to exist and therefore a best fit curve was produced through the points to produce the characteristic curve for the Wells turbine. Taking a full data set, the curve shown in Fig. 5 was obtained.

The solid black line shows the experimental curve while the dashed red line shows the ND torque profile based on the efficiency curve in Fig. 2. It can be seen from this figure that the curve that has been developed has a similar profile to that which is predicted from the

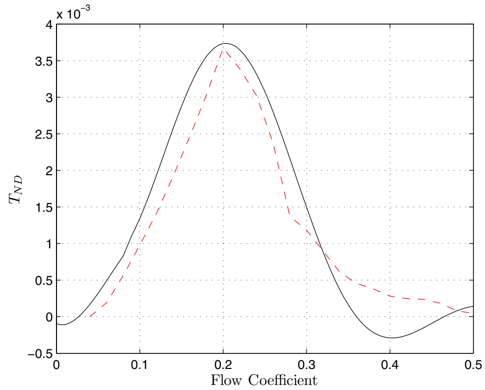

Figure 5: Characteristic ND Torque vs Flow coefficient curve for tested data (black) and efficiency data (dashed red)

efficiency plot shown in Fig. 2. The peak torque is predicted to occur when Φ is equal to 0.2 and after this point aerodynamic stall in the turbine is predicted. Also it can be seen that at low flows a negative torque will be experienced by the turbine which is again predicted in the efficiency plot.

6 Comparison of simulation and experimental test results

This section investigates the simulation of the electrical system shown in Fig. 3 using the characteristic curve developed in the previous section to represent the Wells turbine. The model takes a measured pneumatic power time series from the prototype offshore device which was recorded at the Irish test site. The results from the quarter scale device model are then compared to actual recorded electrical data from the quarter scale OWC WEC prototype device.

In this paper three different sea state conditions are investigated, a high power state, medium state and a low state. The performance of the model is analysed under each of the three conditions. The plots used to demonstrate the results are all given on a per unit basis.

6.1 High power sea state

The pneumatic power profile applied to the model is shown in Fig. 6 at the end of the paper. This profile is a higher power profile at the location where the device is situated. The ratio of the maximum peak power to the average sea state power is 11.62.

The mechanical torque experienced by the Wells turbine is also seen in this plot. The simulated torque is seen to track the measured torque with a reasonable level of accuracy.

The stall region of the turbine can be shown in more detail in Fig. 7 and this highlights that the model predicts this region of operation with a satisfactory degree of accuracy within the level of data sampling.

Fig. 7 shows that a large pneumatic power is experienced between 144s and 146.5s which leads to severe stall occurring in the Wells turbine.

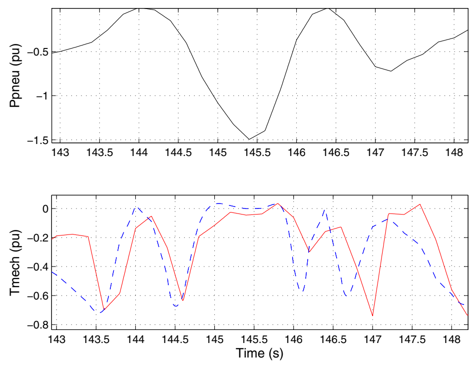

Figure 7: Examination of stall charcteristic of Wells turbine with simulated (blue dashed) and measured (red) torques

A scatter plot of predicted torque versus measured torque is shown in Fig. 8. This plot shows scattered points which indicate the degree of accuracy of the model.

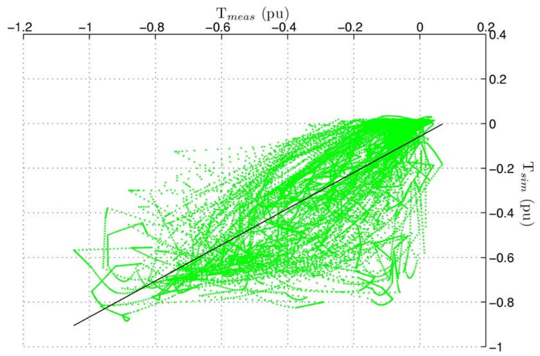

Figure 8: Scatter plot of simulated versus measured parameters (green) and linear fit (black)

A linear fit was plotted through the scatter and this line has a slope of 0.8. This slope indicates that on average the model will have an 80% level of accuracy. The degree of error in the model can be put down to a number of reasons. One of the reasons for scatter in Fig. 8 is due to a phase difference between the measured and simulated torques. This can be seen in Fig. 7. This phase difference has been introduced by the fact that the model is first order and does not take into account higher order aerodynamic effects, for example hysteresis in the turbine.

Other outlying points are due to inaccuracies in the stall region. The prediction of the degree of stall has been seen to be difficult to predict due to a scattering of points in the torque versus flow coefficient curve. It can be seen in Fig. 4 that after the peak torque point that the curve becomes more scattered. Also it should be noted that this curve is formulated by taking a mean torque at each flow coefficient which will lead to certain inaccuracies in instantaneous torque prediction.

Considering the assumptions mentioned and also the slope of the line through the scatter diagram and time series results, the accuracy of the torque prediciton is seen to be of a reasonable level.

Further analysis of the system performance is also seen to be reasonable to a first order approximation with the model seen to predict speed, generated electrical power, armature current and voltage quite accurately throughout. This can be seen in Fig. 9 at the end of the paper.

The figure shows the simulated data in the blue dashed curve while the measured data for speed is in green, generated electrical power is in red, armature current is in magenta and voltage is in cyan. The simulated results are seen to track the experimental results and provide an acceptable representation of the actual systems performance.

6.2 Medium power sea state

In order to investigate if the model is accurate under various sea state conditions further testing was carried out. The following sea state has a power level of medium intensity for the test site with a peak to average ratio of 12.7. This profile would be of medium level in its intensity. Fig. 10 shows the pneumatic profile applied in this case along with the predicted and measured mechanical torques.

The figure again shows that the model can predict the torque experienced by the turbine to a sufficient level of accuracy. Again certain inaccuracies exist in the prediction of torque due to unmodelled aerodynamic effects.

The prediction of electrical parameters was also found to be reasonably accurate. These results are shown in Fig. 11.

6.3 Low power sea state

The final sea state that is tested is a low power sea state. This sea state has a peak to average ratio of 9.63. The pnuematic profile of the sea state along with the turbine torque response is shown in Fig. 12.

The results for the electrical measurements are shown in Fig. 13. The results can again be seen to have a reasonable level of accuracy in this sea state taking into account the simplicity of the model. In this sea state noise on measurements contribute more to inaccuracies. An example of this noise can be seen in the torque plot of Fig. 12 where spikes in the measured torque are seen. This is due to the time derivative of speed that is used in the calculation process for mechanical torque.

These results over various sea states highlight that the characteristic curve developed in Section 2 provides an appropriate model for the Wells turbine despite simplifying assumptions and thus the OWC WEC can be modelled with a reasonable degree of confidence.

6.4 Comparison of energy data

A final analysis of the model is to analyse the predicted electrical and measured electrical energies on a per unit basis. These results are shown in Table 1.

Table 1: Generated electrical energy for various sea states

State	High	Medium	Low
Sim. E_{elec} (p.u.)	1.0	0.67	0.14
Meas. E_{elec} (p.u)	0.89	0.58	0.17

The prediction of electrical energies quantifies the level of accuracy of the model of the system over a period of time. The results shown in Table 1 demonstrate that the model can predict the electrical energy generated from the system within 20% of the actual experimental value. Differences between these values can be put down to simplifying assumptions mentioned earlier coupled with experimenal errors. Examples of such error are in measuring machine frictional coefficient, B_m, inertia, J and also noise that is introduced due to the time derivative of speed which is used in the calculation process. The losses in the electrical power converter have also been neglected.

Whilst a certain degree of error exists in the model the results obtained gives a satisfactory level of prediction of system performance and the model is found to compare favourably with work that has previously been presented on OWC modelling such as in [16].

7 Conclusion

The paper presents the testing and experimental validation of a model for a Wells turbine coupled to a dc generator for a quarter scale offshore OWC WEC prototype. The paper discusses the theory behind the operation of the Wells turbine and uses this theory in modelling the system. Actual test data from an experimental quarter scale prototype device was used to develop a characteristic curve for the performance of the turbine.

A model of the system was developed and the simulated results from this model were compared with actual experimental data from the system for validation purposes. The model was tested under three different types of sea conditions, one of high intensity power density, one of medium intensity power density and one of low intensity power density. Despite simplifying assumptions and experimental error the model was found to predict the mechanical and electrical performance of the system to a satisfactory level of accuracy. This was further demonstrated by examining the measured and predicted electrical energies.

Future work is to be carried out in refining the model and improving its accuracy by taking into account turbine hysteresis and also the different flow regimes that occur in both inflow and outflow conditions.

Further work will also be carried out analysing the electrical system by selecting a more efficient electrical machine and control system. The model that has been developed and validated in this paper can be used to simulate the system with a degree of confidence. This allows for refinements to the electrical system to be simulated.

Acknowledgements

This project has been sponsored by Sustainable Energy Ireland through the Embark Initiative.

The authors would also like to acknowledge the contribution of the Hydraulics and Marine Research Centre at UCC and Ocean Energy Ltd.

References

[1] "Wave energy utilisation in Europe: Current status and perspectives", Centre for Renewable Energy Resources, 2002, pp. 1-28, `http://www.cres.gr/kape/pdf/download/Wave%20Energy%20Brochure.pdf`

[2] "Ocean energy in Ireland", Department of Communications, Marine and Natural Resources, 2005, pp. 1-46, `http://www.marine.ie/NR/rdonlyres/86491414-3E7E-48E5-A0E1-287CA9191C61/0/OceanEnergyStrategy.pdf`

[3] H. Polinder, "Wave energy converters and their impact on power systems", *2005 International Conference on Future Power Systems,* Nov. 2005, pp. 1-9.

[4] M. G. de Sousa Padro, F. Gardner, M. Damon, H. Polinder, "Modelling and test results of the Archimedes wave swing", *2006 Proceedings IMechE,* Vol. 20, Aug. 2006, pp. 855-868.

[5] M. Jasinski, W. Knapp, M. Faust, E. Fris-Madsen, "The power takeoff system of the multi-MW wave dragon wave energy converter", *7th European Wave and Tidal Energy Conference,* Sept. 2007, pp. 1-8.

[6] D. J. Pizer, C. Retzeler, R. M. Henderson, F. L. Cowieson, M. G. Shaw, B. Dickens, R. Hart, "Pelamis WEC-Recent advances in the numerical and experimental modelling program", *5th European Wave and Tidal Energy Conference,* Sept. 2005, pp. 373-378.

[7] A. F. de O. Falcao, "First generation wave power plants: Current status and R&D Requiremants", *Journal of Offshore Mechanics and Arctic Egineering* Vol. 126, Nov. 2004, pp. 384-388.

[8] R. Curran, T. J. T. Whittaker, T. P. Stewart, "Aerodynamic conversion of ocean power from wave to wire", *Energy Conversion Managment,* Vol. 39, No. 16-18, 1998, pp.1919-1929.

[9] P. A. P. Justino, A. F. de O. Falcao, "Rotational speed control of an OWC wave power plant", *Journal of Offshore Mechanics and Arctic Engineering* Vol. 121, May 1999, pp.65-70.

[10] A. F. de O. Falcao, "Control of an oscillating water-column wave power plant for maximum energy production", *Applied Ocean Research* Vol. 24, July 2002, pp. 73-82.

[11] S. Muthukumar, S. Kakumanu, S. Sriram, V. Jayashankar, "Energy storage considerations for stand alone wave energy plant", *IEEE Conference on Electric Machines and Drives,* May 2005, pp. 193-198.

[12] M. Molinas, O. Skjervheim, P. Andreasen, T. Undeland, J. Hals, T. Moan, B. Sorby, "Power electronics as grid interface for actively controlled wave energy converters", *IEEE International Conference on Clean Electrical Power*, May 2007, pp.188-195.

[13] S. Muthukumar, S. Kakumanu, S. Sriram, R. Desai, A.A.S. Babar, V. Jayashankar, "On minimizing the fluctuations in the power generated from a wave energy plant", *Proceedings of IEEE International Conference on Electric Machines and Drives* May 2005, pp.178-185.

[14] D. Ravi Kiran, A. Palani, S. Muthukumar, V. Jayashankar, "Steady grid power from wave energy", *IEEE Transactions On Energy Conversion* Vol. 22, No. 2, June 2007, pp.539-540.

[15] D.L. O' Sullivan, A. W. Lewis, "Generator selection for offshore oscillating water column wave energy converters", *European Power Electronics Conference 2008* , Sept 2008, pp. 1790-1797.

[16] R.G.H. Arlitt, K. Tease, R. Starzmann, J. Lees, "Dynamic System Modeling of an Oscillating Water Column Wave Power Plant based on Characteristic Curves obtained by Computaional Fluid Dynamics to enhcance Engineered Reliability", *7th European Wave and Tidal Energy Conference,* Sept. 2007, pp. 1-8.

[17] D.V. Evans, R. Porter, "Hydrodynamic characteristics of an oscillating water column device", *Applied Ocean Research* , Vol. 17, May 1995, pp. 155-164.

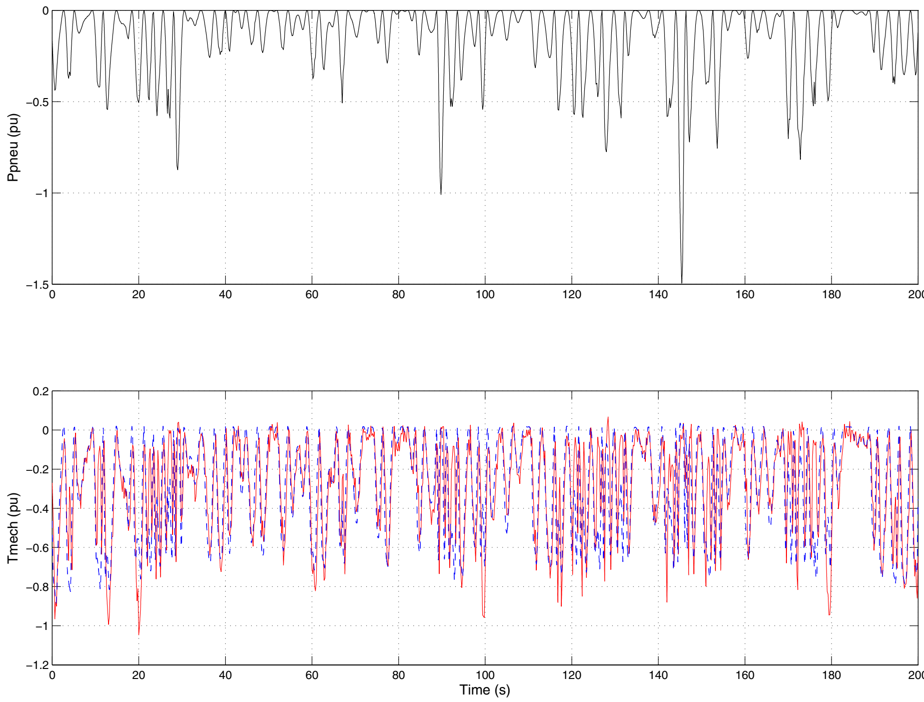

Figure 6: Pnuematic power profile with simulated (blue dashed) and measured (red) torques for high level sea state

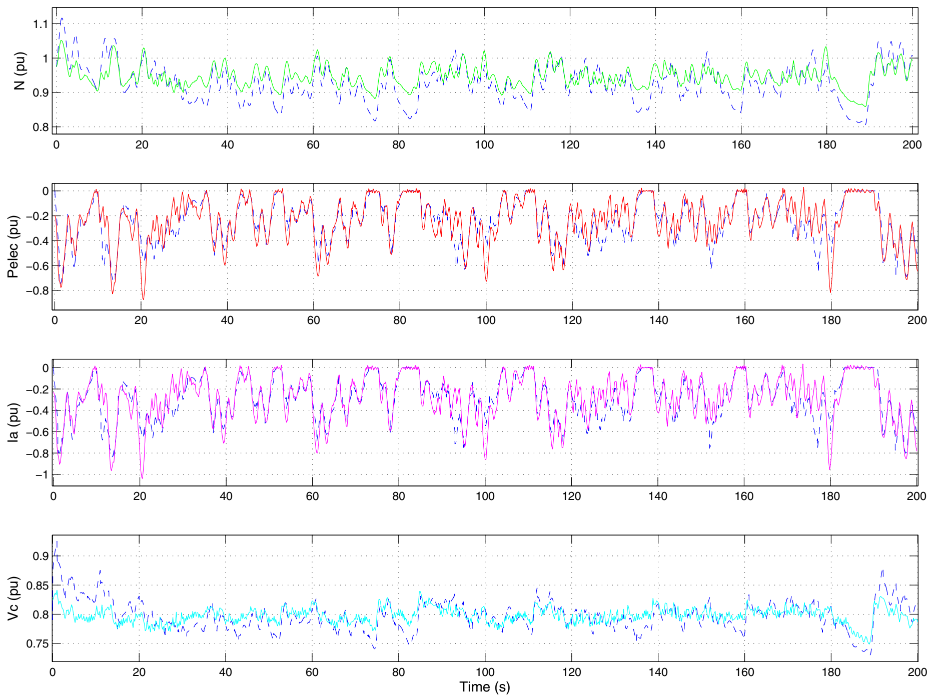

Figure 9: Electrical parameters simulated (blue dashed) and measured (green,red,magenta,cyan)for high level sea state

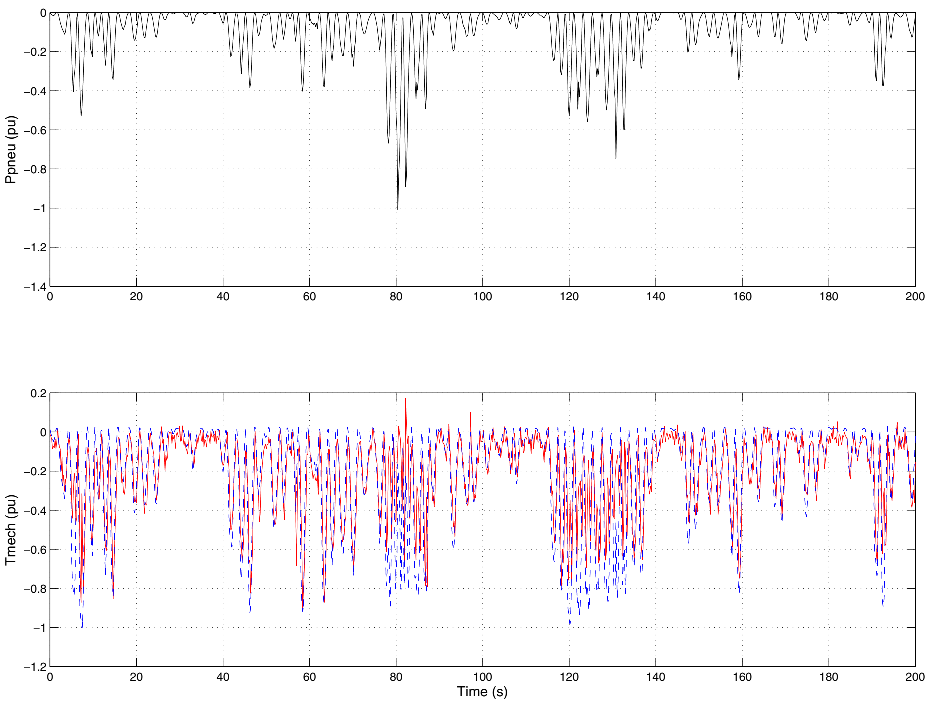

Figure 10: Pnuematic power profile with simulated (blue dashed) and measured (red) torques for medium level sea state

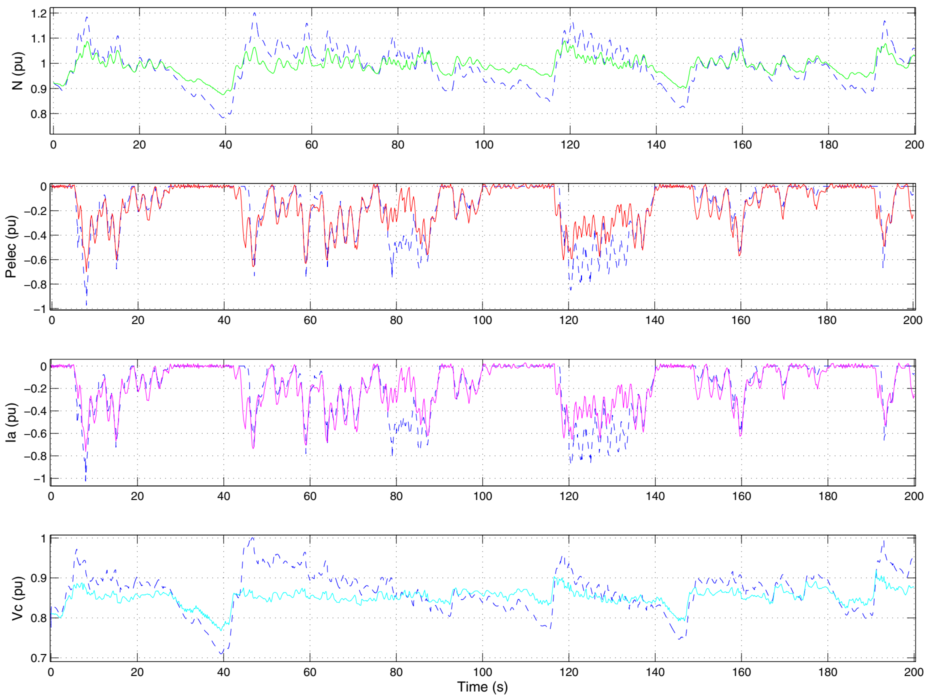

Figure 11: Electrical parameters simulated (blue dashed) and measured (green,red,magenta,cyan) for medium level sea state

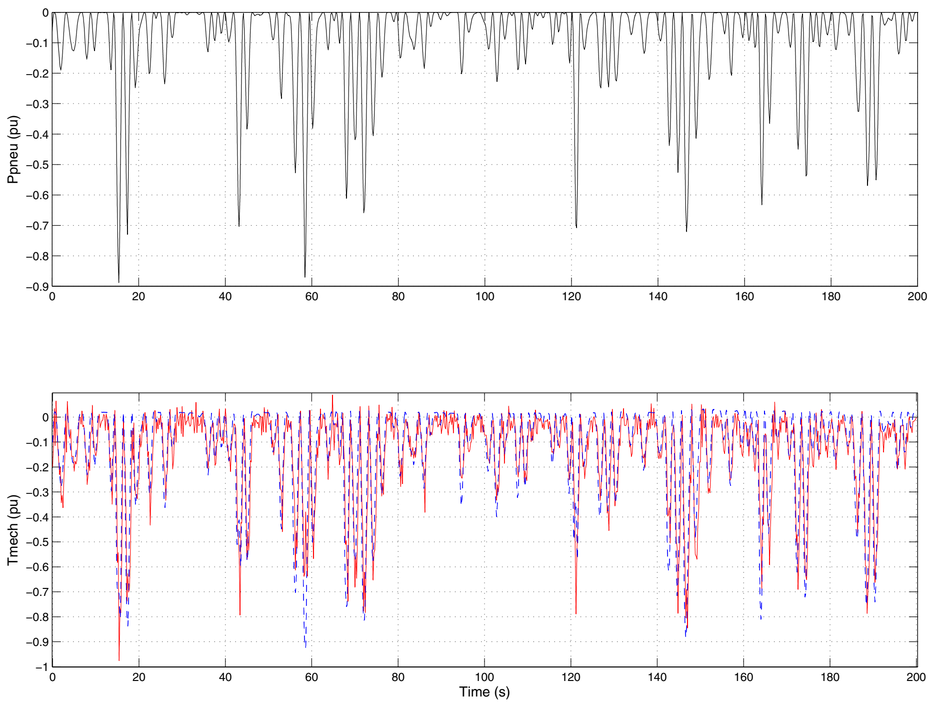

Figure 12: Pnuematic power profile with simulated (blue dashed) and measured (red) torques for low level sea state

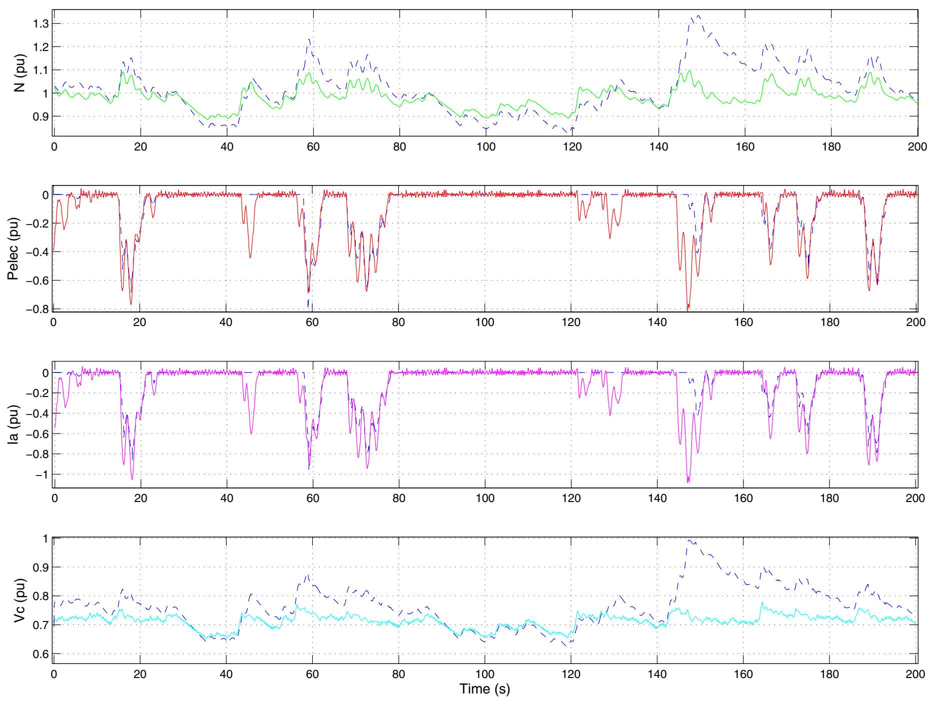

Figure 13: Electrical parameters simulated (blue dashed) and measured (green,red,magenta,cyan) for low level sea state